Forsythia Flower as Natural Photosensitizer for Dye-sensitized Solar Cells

Zhenghao Liu[1], Jinjin Zhao[1]*, Liyu Wei[1], Bing Qiao[2]*, Jiao Liu[3]*, Wenna Wang[1], Xiaoyan Du[1], Tengkun Li[1], Lei Wang[1]

1School of Materials Science and Engineering, The Key Laboratory for Health Monitoring and Control of Large Structures , Shijiazhuang Tiedao University, 17 Northeast, Second Inner Ring, Shijiazhuang, 050043, China
2 First Medical Oncology, Han Gang Hospital,188 Nonglin Road, Handan,056001,China
3TCM Pharmacology Laboratory, Hebei Traditional Chinese Medicial College, Shijiazhuang 050200, China

Abstract. Pigments of Forsythia flowers were facilely extracted. Ultraviolet-visible (UV-Vis) absorption spectra of nanocrystal TiO_2 film sensitized by Forsythia dyes, and photoelectric property of natural dye-sensitized solar cells (DSSCs) confirmed that the strong capacity of Forsythia visible light absorption, and the short-circuit current density and the photoelectric conversion efficiency of forsythia DSSC is 2.07mA/cm^2 and 0.79%, respectively, attributed by energy level well matching of forsythia dyes excited states with the TiO_2 conduction band energy level.

1 Introduction

With increasing global energy consumption and environmental issues, the fabrication of low cost and high efficiency photovoltaic cells has attracted intense research interest in recent years,[1~3] Since Grätzel developed dye-sensitized solar cells (DSSCs), a new type of solar cells[1] in 1991. DSSCs are composed of the porous semiconductor electrode absorbed dye, the counter electrode and the electrolyte. The photoanode is prepared by adsorbing a dye into a porous TiO_2 layer. By this approach, the dye enables the generation of electricity with visible light, extending the semiconductor's performance to collect photons at lower energy.[4] DSSCs usually employ ruthenium(II) polypyridinic complexes as sensitizers of wide band gap semiconductors, although the energy conversion can also be achieved by natural dyes. But those synthetic dyes are expensive and complicated Purification. Alternatively, natural dyes can be used for the same purpose with an acceptable efficiency.[5-12] Recent literature indicates that DSSC with anthocyanin has shown better performance than the DSSC using chlorophyll dye. The DSSC with the dye mixture exhibits better performance than individual dye.[13] Here, DSSCs were prepared using natural dyes extracted from Forsythia as sensitizers. We firstly assembled forsythia as a sensitizer into solar cells, studied the performance of forsythia sensitized photovoltaic solar cells and the stability of device performance.

2 Experimental Section

2.1 Chemicals

Titanium tetrachloride (99.5%), Ethanol (98%), Nitric acid (65%) were purchased from Sinopharm Chemical Reagent Co., Ltd; F127 was purchased from Sigma-Aldrich, Inc. Polyethylene glycol (PEG; 20000 in molecularweight) was purchased from J&K. The sensitizer N719 (Cis-di(thiocyanato)-N, N-bis(2, 2 ' - bipyridyl-4,4 ' - dicarboxylate)- Ru(II) bis-tetrabuty lammonium), electrolyte, surlyn film were purchased from Yingkou Opvtech New Energy Co., Ltd.

2.2 Synthesis of the TiO_2 film and fabrication of Forsythia -Dye Sensitized Solar Cells (FDSC)

2.2.1 Synthesis of TiO_2 nanoparticles

TiO_2 nanoparticles were synthesized as the following method. 2.97g F127 was firstly dissolved in 36.88g ethanol at 40℃ for 30 minutes to form a clear solution. Then 3.4g $TiCl_4$ was added to the obtained solution. The precursor solutions were placed into a Teflon-lined stainless steel autoclave (100 mL in capacity) after stirring 8h under 40℃. The autoclave was placed in an oven at 160℃ for 16h. Subsequently, the products were filtered, washed and dried at 80℃. Finally, the powders were sintered at 610℃ for 10 minutes after being kept at 300℃ for 90 minutes and 500℃ for 240 minutes. During the whole process, the heating rate was kept at a constant of 2℃/min. After sintering, the products were dispersed using deionized water and nitric acid (65%) until the pH of the solution reached to about 2.[14]Then the mixture solution was vigorous stirred at 80℃ for 8 hours to obtain TiO_2 nanoparticles.

2.2.2 Preparation of Mesoporous TiO_2 films

FTO conductive glass sheets (SnO_2:F coated glass, FTO, sheet resistance: 8 ohm/sq) were first cleaned in a detergent solution using an ultrasonic bath for 15~30 min, rinsed with water, ethanol, acetone and then dried with nitrogen. The mesoporous TiO_2 films with a thickness of 8~15 μm were prepared by the doctor-blade method. First of all, the TiO_2 paste was made with the TiO_2 nanoparticles synthesized in section 2.1. Briefly, 0.8g TiO_2 was added in a mixed solution of ethanol/deionized water (3:1) and treated using ultrasonic for 30 minutes after the addition of PEG aqueous which acted as the pore-forming material. Then they were grinded into ropiness in agate mortar. A mask, with a window encompassed by 3M scotch tape, was used to define the

5mm×5mm area which was used to spread the paste dropped one edge of the window with a glass slide on the FTO conductive glass. Subsequently, the as-prepared TiO$_2$ films were sintered in air with the heating rate of 2℃/min to 300℃ for 30 min, 500℃ for 60 min.

2.2.3 Preparation of natural dye sensitizers

The natural dyes were prepared by the following steps: Forsythia flowers were washed with water and dried at 50 ℃for 15min. 2 g fresh Forsythia flowers were crushed using a mortar and immersed in 10ml ethanol solution at room temperature in the dark for 3 hours, and then solid residues were filtrated out. The resulting filtrates were used as sensitizers.

2.2.4 Preparation of Forsythia dye-sensitized solar cell

The mesoporous TiO$_2$ films were sensitized with Forsythia dye or N719 dye by direct adsorption. Firstly, the as-prepared TiO$_2$ films were heated to 80℃ and immersed in the Forsythia dye and N719 ethanol solution （0.5mM）for 24 h, respectively. After rinsing the film in solution by ethanol and drying, the desired mesoporous TiO$_2$/ Forsythia dye film and TiO$_2$ / N719 electrodes were obtained.

The photovoltaic cells were assembled with the mesoporous TiO$_2$/Forsythia dye film or TiO$_2$/N719 photoelectrode, Pt coated counter electrode, and 60μm thick sealing material (OPV-SN-60). Commercially available electrolyte of I$_3^-$/I$^-$ was injected into the space between the photoelectrode and counter electrode.

2.3 Characterization

UV-Vis absorption spectras were recorded with a Shimadzu UV-2550 (300－600 nm: xenon lamp, 300 W; 600－900 nm: tungsten-halogen lamp, 150 W). The infrared spectra of functional groups on forsythia pigment analysis were taken on a Fourier transform infrared (FT-IR) spectrometer (Nicolet 330, Thermo, USA). XRD patterns were obtained using D8 Advance (Germany) diffractometer with Cu Kα radiation (40 kV and 40 mA) with the scanning rate of 4°min-1 for wide angle test sincrement over the Bragg angle range of 20–90°. The N$_2$ sorption measurements were performed using Micromeritics Tristar 3000 for mesoporosity and Micromeritics ASAP 2020 porosimeters and microposity at 77 K, respectively. The mesoporous specific surface area and the pore size distribution were calculated using the Brunauer－Emmett－Teller (BET) methods. SEM (Scanning Electron Microscopy) analysis was performed on a Hitachi-S-4800 electron microscope. The photocurrent-voltage (J－V) characteristics of the solar cells were measured using a Keithley 2400 Source under illumination of a simulated sunlight (AM1.5, 100 mW/cm^2) provided by a solar simulator (Newport 69907) with an AM 1.5 filter. Light intensity was adjusted with an NREL-calibrated Si solar cell with a KG-2 filter for

approximating 1 sun light intensity. The incident photon-to-current efficiency (IPCE) was measured in DC mode with a 1/4 m double monochromator (Crowntech DK242), a multi-meter (Keithley 2000), and two light sources depending on the wavelength range required (300－600 nm: xenon lamp, 300 W; 600－900 nm: tungsten-halogen lamp, 150 W). The monochromatic light intensity for IPCE efficiency was calibrated with a reference silicon photodiode.

3 Results and discussion

3.1 Structural characterization

SEM and TEM image of TiO$_2$ nanoparticles were shown in Fig.1. It shows that the diameter of the prepared TiO$_2$ particles was about 20–50 nm. Fig.2 shows the XRD patterns of the TiO$_2$ nanoparticles. The TiO$_2$ particles
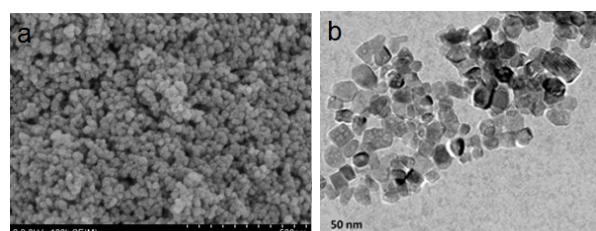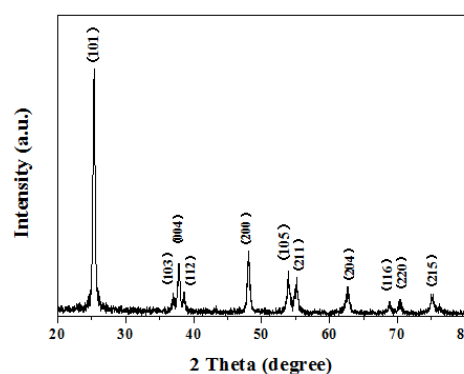

Fig.1 SEM and TEM image of TiO$_2$ nanoparticles

Fig.2 XRD (PDF:73-1764) patterns of TiO$_2$ nanoparticles

exhibited diffraction peaks at 2θ values of 25.51°, 37.08°, 37.89°, 38.714°, 48.18°, 54.05°, 55.403°, 62.96°, 69.01°, 72.45°, 75.29°, corresponding to the (101), (103), (004), (112), (200), (105), (211), (204), (116), (220), (215) crystal planes of anatase TiO$_2$ (I4$_1$/amd, JCPDS 73-1764). The observed XRD results are well matched with already reported literature.[18]

Nitrogen sorption isotherms of the TiO$_2$ nanoparticles and the corresponding pore size distribution curve (inset) are shown in Fig.3. The isotherms of TiO$_2$ nanoparticles exhibit a TiO$_2$ nanoparticles has type-H1 hysteresis loop, characteristic of mesoporous materials, with clear adsorption and desorption jumps at 0.6 and 0.9.The specific surface area of 45.24 m²/g and pore volume of 0.16 cm³/g, an average pore diameter of 10.4 nm, which are enough for the high capacity enrichment of Forsythia flower dye.
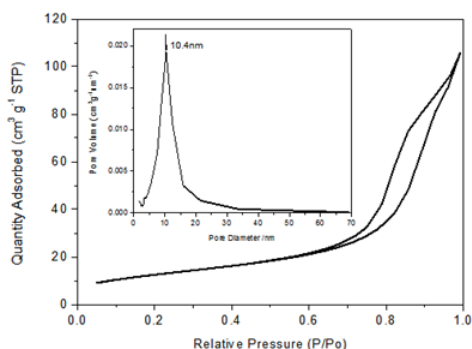
Fig.3 N$_2$ adsorption-desorption isotherms and the corresponding pore diameter distribution curves of TiO$_2$ nanoparticles
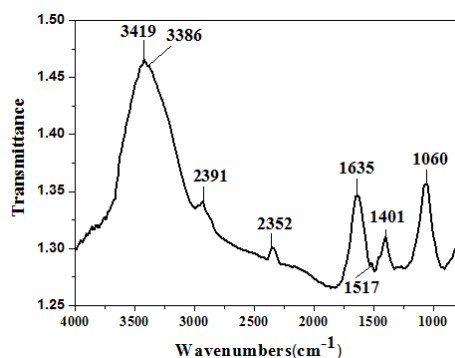

Fig.4 the FT-IR absorption spectrum of forsythia flower pigment

The FT-IR absorption spectrum of forsythia flower pigment was shown in Fig.4. It is noted that pigment's molecular structure found in forsythia flowers in accordance with the report[19]. Fig 5 showed molecular formula of forsythia phillyrin and forsythiaside glycosides.
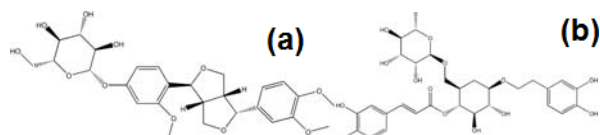

Fig.5 the main components of forsythia flower pigment: molecular formula of forsythia phillyrin (a) and forsythiaside glycosides (b)

Fig.6 shows the UV–vis absorption spectra of nanocrystalline TiO$_2$ film (black) and nanocrystalline TiO$_2$ film sensitized by Forsythia (red). The absorption onset for TiO$_2$ is approximately 450 nm, while the absorption onset of sensitized TiO$_2$ film is about 665 nm. The difference in the absorption characteristics is due to nanocrystal TiO$_2$ film sensitized by Forsythia. Fig.7 reports a plot of $(Ahv)^2$ versus hv (A=absorbance, h=Planck's constant, and v=frequency), from which it is possible to extrapolate the slope near the absorption edge and extract the band gap energy.[15] The fits yielded 1.81eV for TiO$_2$@Fo-dye, which is lower than the band gap value of TiO$_2$ (Eg=3.2eV), due to the density of state of TiO$_2$/Fo-dye contributed by the surface states of Fo-dye.
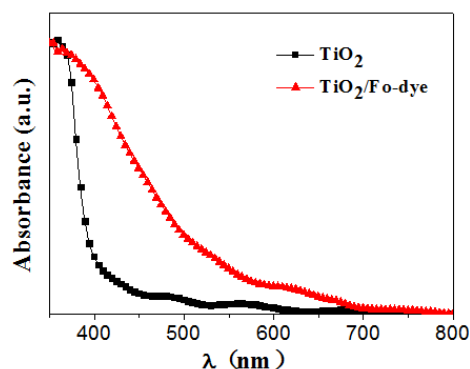

Fig.6 UV-vis absorption spectra of nanocrystalline TiO$_2$ film and nanocrystalline TiO$_2$ film sensitized by Forsythia
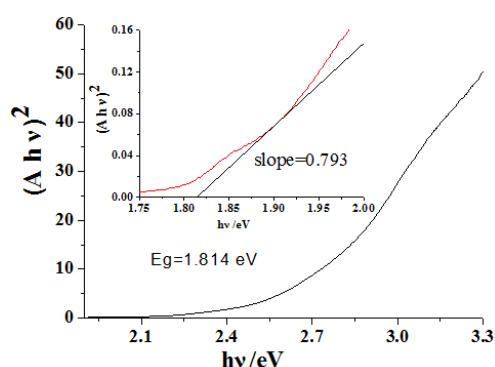

Fig.7 Plots of $(Ahv)^2$ against the photon energy (hv) for TiO$_2$/Fo-dye

As observed in Fig.8, it shows the intramolecular charge transfer (ICT) from donor to acceptor/anchoring group. the pattern of the HOMOs and LUMOs are beneficial for the photoexcitation electrons injection. The dye has considerable contribution to the LUMOs which could lead to a strong electronic coupling with TiO$_2$ surface and thus improved the electron injection efficiency, and subsequently enhance the short-circuit current density Jsc.[16]
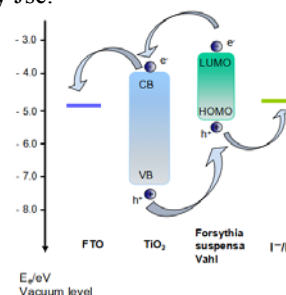

Fig.8 A schematic showing the relative band energy levels for charge transfer in the FTO/TiO$_2$/Forsythia electrolyte.

The photocurrent–voltage curves of the DSSCs based on Forsythia in Fig.9a was measured under light irradiation with intensity of 100 mW/cm^2. The photovoltaic parameters of DSSCs such as J$_{SC}$, V$_{OC}$, FF and PCE are listed in Fig.9a. The PCE of DSCs based on Forsythia reaches 0.79%, which is higher than that of Rosella (PCE=0.37%), Blue pea(PCE=0.05%) Mixed rosella–blue pea (PCE=0.15%).[17] Fig.9b shows that the IPCE curves respond from 400 nm to 600 nm, which has

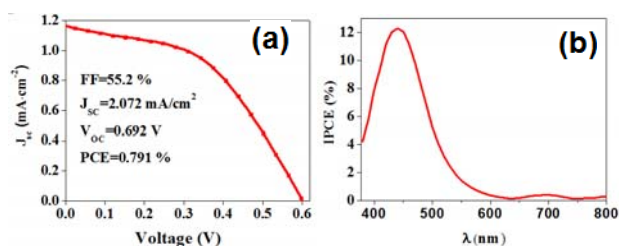a greatest IPCE performance in general, with the maximum at 440 nm.

Fig.9 (a) photocurrent density-voltage (J-V) and (b) Incident-photon-to-current conversion efficiency (IPCE) photocurrent density-voltage (J-V) curves of the DSCs

For the stability of forsythia dyes device, we measured the photocurrent–voltage curves of the DSSCs based on Forsythia under light irradiation with intensity of 100 mW/cm^2 130 times. As observed in Fig.10 (a), the efficiency is maintained at between 0.61% -0.71% which indicating that the pigment from the forsythia as a sensitizer is stable. Fig.10 (b) shows the UV–vis absorption spectra of dyes storaged in different temperature. It was found that the absorption peak of dyes storaged in different temperature are the same, which indicates that the dye is stability to temperature and has good stability.
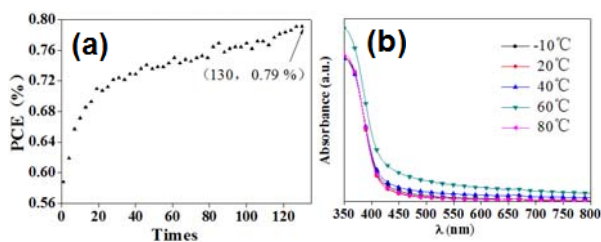

Fig.10 (a) relation curve of Forsythia's photoelectric conversion efficiency and the test number of times; (b) UV-vis absorption spectra of dyes treated in different temperature

4 Conclusions

Ultraviolet-visible (UV-vis) absorption spectra of forsythia dyes, and photoelectric performance of DSSCs showed that the visible absorption ability, the short-circuit current and the photoelectric conversion efficiency of forsythia DSSC, and forsythia dyes excited states of LUMO and HOMO energy levels with the TiO$_2$ conduction band energy level and electrolyte oxidation reduction. The photoelectric conversion efficiency of Forsythia DSSC reached 0.79%. Natural dyes can be used for the same purpose with a good efficiency, and moreover natural dye performance is stable, low-cost, environment-friendly.

References

[1] M. Grätzel, *Acc. Chem. Res.* **42**, 1788 (2009).
[2] T. T. Wang, P. Raghunath, Y. F. Lu, Y. C. Liu, C. H. Chiou, M. C. Lin, *Chem. Phys. Lett.* **510**, 126 (2011).
[3] Q. Wang, *Nature*, **494**, 403 (2013).
[4] G. Calogero, G. Di Marco, *Sol. Energy Mater. Sol. Cells*, 92, 1341 (2008).
[5] K. Tennakone, G. R. R. A. Kumara, A. R. Kumarasinghe, P. M. Sirimanne, K.G.U. Wijayantha, *J. Photochem. Photobiol. A.*, **94**, 217 (1996).
[6] S. Hao, J. Wu, Y. Huang, J. Lin, *Sol. Energy*, **80**, 209 (2006).
[7] Y. Amao, T. Komori, *Biosensors Bioelectron.* 19, 843 (2004).
[8] A. S. Polo, N. Y. Iha, *Sol. Energy Mater. Sol. Cells*, **90**, 1936 (2006).
[9] C. G. Garcia, A. S. Polo, N. Y. Iha, *J. Photochem. Photobiol* A., **160**, 87 (2003).
[10] G. P. Smestad, *Sol. Energy Mater. Sol. Cells*, 55, 157 (1998).
[11] G. R. A. Kumara, S. Kanebo, M. Okuya, B. Onwona-Agyeman, A. Konno, K. Tennakone, *Sol. Energy Mater. Sol. Cells*, **90**, 1220 (2006).
[12] N.J. Cherepy, G.P. Smestad, M. Grä̈tzel, J.Z. Zang, J. Phys. Chem. B101 (1997) 9342.
[13] M. M. Noor, M. H. Buraidah, M. A. Gareem, S. R. Majid, A. K. Arof, *Electrochimica Acta*,**121**, 159 (2014).
[14] A. B. F. Martinson, T. W. Hamann, M. J. Pellin and J. T. Hupp, *Chemistry - A European Journal*, **14**, 4458 (2008).
[15] M. Shalom, J. Albero, Z. Tachan, E. Martínez-Ferrero, A. Zaban, E. Palomares, *J. Phys. Chem. Lett.*, **1**, 1134 (2010).
[16] A. Fitri, A. T. Benjelloun, M. Benzakour, M. Mcharfi, M. Hamidi, M. Bouachrine, *Spectrochimica Acta Part A-Molecular and Biomolecular Spectroscopy*, **132**, 232 (2014).
[17] K. Wongcharee, V. Meeyoo, S. Chavadej, *Sol. Energy Mater. Sol. Cells*, **91**, 566 (2006).
[18] J. Zhao, J. Zhang, W. Wang, P. Wang, F. Li, D. Ren, H. Si, X. Sun, F. Ji, Y. Hao, *Dalton Trans.* **43**, 16588 (2014).
[19] B. Luo, J. Z. Zhang, *Chinese Joumal of Experimental Traditional Medical Fomulae* **19**, 143-146 (2013).